Experimental Determination of High-Acceleration Shock Characteristics of Industrial Marine Fenders

David, N. V.[*]*, Adelin Khairina, M. S.*
School of Mechanical Engineering, College of Engineering,
Universiti Teknologi MARA, 40450 Shah Alam, Selangor, MALAYSIA
[*]*davidfkm@uitm.edu.my*

Vipin Gopan
Department of Mechanical Engineering,
St. Thomas College of Engineering and Technology,
689521 Chengannur, Kerala, INDIA

ABSTRACT

Engineering systems are often subject to complex loading mechanisms including accelerated mechanical shock during transportation, handling, and operations. Shock can be understood as a drastic, irregular change in acceleration experienced by an object due to impact at a very short period. This paper presents a preliminary study of the crashworthiness properties of in-service industrial marine fenders (or bumpers) intended for shock energy absorption. The peak accelerations (G_{peak}) of the test specimens are experimentally measured and compared to theoretical estimations. The energy absorptions and impact forces of the test specimens are calculated using analytical formulations. The effects of introducing tubular through-holes in the specimens on the resulting peak accelerations and thereby the shock energy absorbing capacities are also investigated. Test specimens of thicknesses ranging between 10 mm and 30 mm are subjected to half-sine shock waves between 50G and 70G, which are generated by dropping a 5-kg payload from different heights ranging from 150 mm to 280 mm onto a padded shock seat for a pulse duration between 5 and 8 ms. The analytically determined G_{peak} agrees well with the experimental values. It is found that the through-holes specimens with lower G_{peak}, resisted smaller impact forces and absorbed up to 12% lesser energy per unit mass than their solid counterparts.

ISSN 1823-5514, eISSN 2550-164X

https://doi.org/10.24191/jmeche.v12i1.24635

Received for review: 2023-07-26
Accepted for publication: 2023-10-18
Published: 2023-11-15

Keywords: *Mechanical Shock; Crashworthiness; Marine Fender; Energy Absorption; Half-Sine Wave; Impact Force*

Introduction

Shock is an incident of rapid high acceleration that may come in the form of impact and cause structural damage to the components exposed to it. Efficient energy absorption by materials and components can protect them from sudden shock at peak acceleration, i.e. G_{peak} (e.g., [1]-[3]). Crashworthiness properties of a material system such as a marine fender (see Figure 1a) are essential for product designing and life cycle analysis [4]. High shock impacts induce microcracks that can grow and propagate resulting in major fracture of the material system and industrial components (e.g., [5]-[8]). Industries pertinent to crashworthy component applications therefore routinely employ measures to lessen the post-impact damages. Mechanical shock testing experiments are designed to evaluate the capability of crashworthy components to absorb impact energy at high shock accelerations by dropping them from a certain height and measuring the resulting G_{peak}. This usually involves prior determination of the shock pulse durations and heights as the input parameters for the test (e.g., [9]-[10]). The G_{peak} and velocity change experienced by the test specimens are measured using an accelerometer and used to theoretically determine the impact force and maximum energy absorption of the specimens. G_{peak} can also be analytically calculated. In this case, the principle of conservation of energy is normally invoked to relate test parameters including drop height, h, and pulse duration, dt, to the impact force and energy absorption of the specimens (e.g., [11]-[12]). The following expression for G_{peak} is derived based on the assumption that the test system is conservative and there is no rebound of the mass during the impact (see Appendix A for derivation):

$$G_{peak} = \frac{\pi\sqrt{gh}}{dt\sqrt{2}} \tag{1}$$

The impact force, F, can be determined from the velocity change, dv, specimen mass, m, and dt as follows:

$$F = m\left(\frac{dv}{dt}\right) \tag{2}$$

Potential energy, U, of the mass at a height h from where the mass is dropped is assumed to be fully transformed to kinetic energy, T, just as it impacts the programmer at its peak velocity (see Figure 1b). Using this assumption, the maximum specific energy absorption of the specimens, SEA,

can be determined from the maximum velocity, v_{max}, and dt as follows (see Appendix A for derivation):

$$\text{SEA} = \frac{1}{2}\left(\frac{G_{peak} \times dt}{2\pi}\right)^2 \tag{3}$$

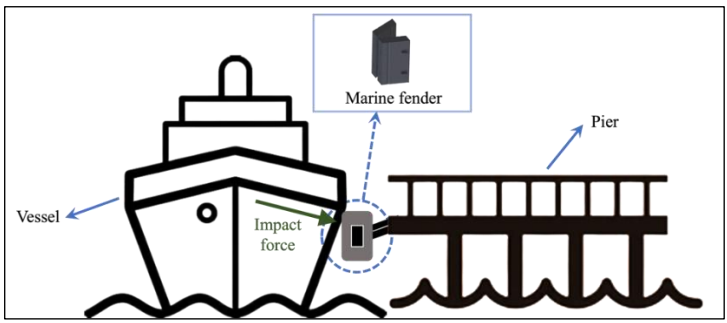

Figure 1a: Illustration of a crashworthy marine fender application: A vessel berthing at a pier and the impact force direction on the marine fender

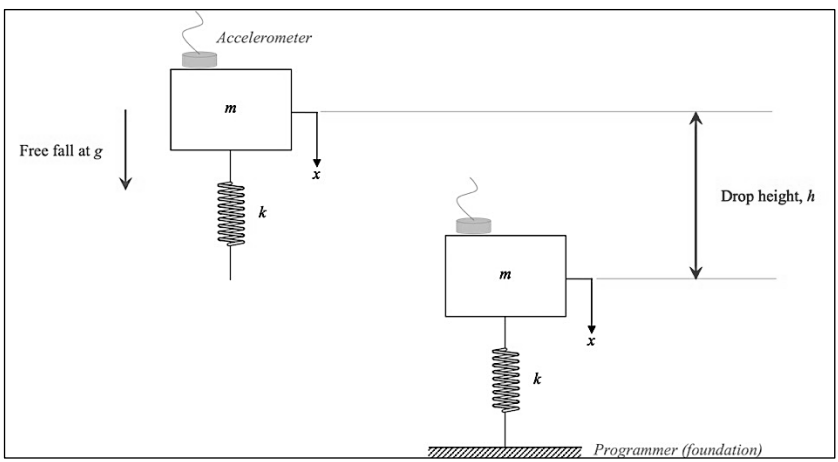

Figure 1b: Schematic modeling of a test specimen; (a) during free fall, and (b) upon impact on programmer to simulate the mechanical shock experienced by the specimen

The crashworthy properties of a marine fender including its G_{peak}, and the related F and SEA are dependent on a variety of factors including the type

and make of the fender, vessel tonnage, berthing mechanism and impact velocity, dynamic factors, and the geometrical setup of the fender installation at the docking terminal [13]. Various types of fenders for different kinds of loading applications have been studied (e.g., [14]-[16]). Marine fenders are used between 10 and 40 years in general. The physical, thermal, and mechanical properties of marine fenders particularly those made of rubber change over time from their first commercial usage due to repeated impacts and aging due to environmental conditions (e.g., seawater absorption, corrosion, UV radiation). The changes in these properties in turn affect the crashworthiness performance of the fenders in later years as reported in major marine industry standards and guidelines (e.g., [17]-[18]). However, the changes in the crashworthiness of in-service marine fenders because of prior impact and aging are not generally investigated. The present study is novel in this aspect.

In this study, the crashworthiness of an industrial marine fender block of the element type is experimentally determined. The as-is test specimen is then modified by introducing tubular through-holes to investigate the combined effects of reduced mass and geometrical change on their G_{peak} levels and thereby the shock energy absorbing capacities. This modification is intended to simulate the effects of high acceleration shock experienced by the fenders and other material systems in real-world applications (e.g., [19]-[22]). The results are further analyzed using the above theoretical formulations to determine the impact forces and SEA of the original and modified specimens.

Methods

Specimen preparation

The test specimens for the purpose of this study are sampled from an industrial-grade rubber fender (or, bumper) contributed by Malaysia Marine and Heavy Engineering Sdn. Bhd. in its pre-used condition. This marine bumper (MB) block, which is an element fender type intended for berthing oil and gas vessels, is cut into the required test dimensions using a horizontal band saw. The solid MB specimens (MB-S) have a common width of 100 mm and a length of 150 mm but differ by their thicknesses, i.e. 10 mm, 20 mm, and 30 mm which are labeled as MB1-S, MB2-S, and MB3-S, respectively. The benefit of introducing hollow sections in a solid fender on its energy absorption capability is described in [15]. The test specimens in the present study are therefore further varied by adding hollow sections of 5-mm diameter through holes, which are drilled using the ERLO TSR-32 column drilling machine. This set of specimens is labeled as MB-H. The placements of the symmetrical hollow sections are indicated in Figure 2. The specimens are shown in Figure 3 and their respective masses are listed in Table 1. It is to be noted that specimen MB2-H is heavier than MB2-S. This implies density changes within

this specimen that could have occurred during the operational service of the MB block.

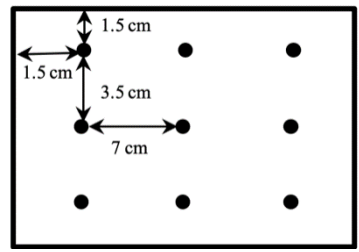

Figure 2: The positions of hollow sections in specimens MB-H

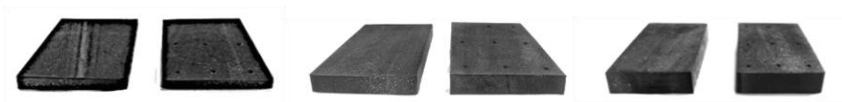

Figure 3: The array of test specimens
(*Can be viewed in 3D at https://xr.plus/yad*)

Table 1: Masses of the marine bumper specimens

Specimen ID	MB1-S	MB1-H	MB2-S	MB2-H	MB3-S	MB3-H
Mass (kg)	0.226	0.184	0.387	0.406	0.590	0.568

Experimental procedure

Trial rounds of mechanical shock testing are first conducted on pilot specimens to identify the input parameters, i.e. the combinations of height (h) and pulse duration (dt), that would provide a range of desired peak acceleration, G_{peak}, levels, i.e. 50G, 60G, and 70G. These levels correspond to the berthing energies that are normally encountered by industrial marine fenders intended for oil and gas vessels [17]. The identified input parameters are listed in Table 2.

The specimens for both pilot and actual test rounds are subjected to half-sine shock waves, which are generated by dropping a 5-kg payload onto a padded shock seat in an ASLI SS-5 high acceleration mechanical shock tester based on the MIL-STD 810 standard (Method 516, Procedure 1) [23] (see Figure 4). Specimens for the actual test rounds are subjected to three drops each at the identified input parameters.

The experimentally measured peak accelerations (G_{peakEx}), dv, and dt for each specimen for all the three drops are logged. The average G_{peakEx} values are compared to analytical peak accelerations, G_{peakAn}, that are determined

using Equation 1. The impact forces and energy absorptions of the specimens are then determined from Equations 2 and 3, respectively.

Table 2: Input parameters identified for each test specimen

Desired G_{peak}		Specimens					
		MB 1 (t = 10 mm)		MB 2 (t = 20 mm)		MB 3 (t = 30 mm)	
G	m/s^2	H (mm)	dt (ms)	h (mm)	dt (ms)	h (mm)	dt (ms)
50	490.5	170	8	150	8	160	7
60	588.6	220	6	180	6	200	6
70	686.7	280	6	240	5	240	5

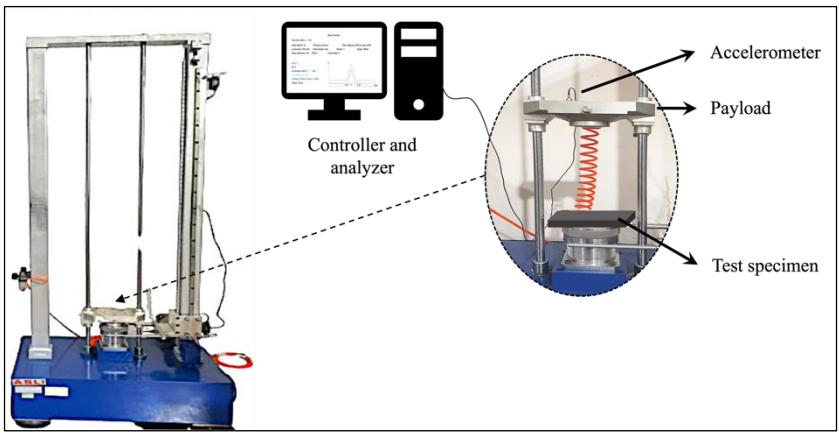

Figure 4: Experimental setup of the mechanical shock tester

Results and Discussions

Validation of input parameters

The input parameters listed in Table 2 need to be validated in producing the desired accelerations on the specimens. Table 3 lists the output G_{peakEx} values for all the specimens in response to the respective input parameters during the trial rounds. The median G_{peakEx} values at each desired acceleration are shown in Figure 5. The standard deviations of G_{peakEx} at the desired accelerations of 50G, 60G, and 70G are 40.7 m/s^2, 35.3 m/s^{2,} and 16.8 m/s^2, respectively. This represents a variation of not more than 8% from the intended input accelerations onto the specimens.

Table 3: Trial round experimental peak accelerations (G_{peakEx}) in response to the input parameters listed in Table 2

Desired G_{peak}		G_{peakEx} (output)					
G	m/s^2	MB1-S	MB1-H	MB2-S	MB2-H	MB3-S	MB3-H
50	490.5	527.3	516.9	581.2	470.4	504.7	473.8
60	588.6	644.5	611.6	590.4	543.4	565.1	594.5
70	686.7	720.4	711.4	674.3	697.0	694.3	685.3

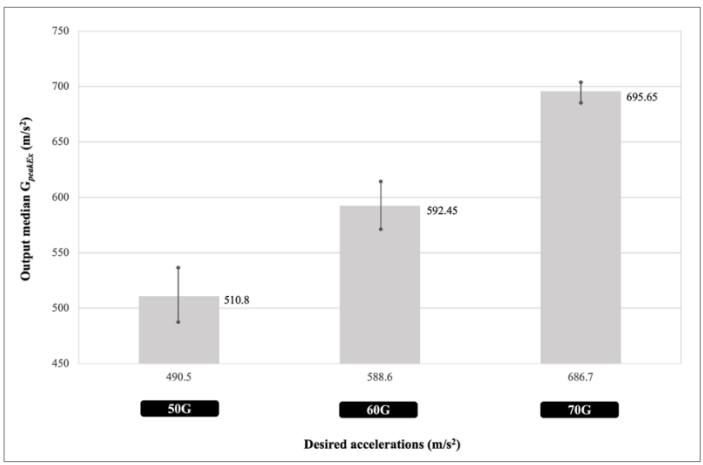

Figure 5: Median G_{peakEx} values (indicated at top right corner of each bar) at the desired accelerations of 50G, 60G, and 70G

Experimental and analytical shock acceleration responses

The shock acceleration responses of the specimens at 50G, 60G, and 70G inputs during the actual drop tests, i.e. G_{peakEx}, are shown in Figures 6, 7, and 8 for specimens MB-1, MB-2, and MB-3, respectively. These figures also include the corresponding values of G_{peakAn}. The correlation strength between G_{peakEx} and G_{peakAn} is indicated by the R^2 values.

The R^2 values, which lie between 0.9848 and 1, signify a strong correlation between G_{peakEx} and G_{peakAn}. This indicates that the analytically determined shock accelerations agree well with that of the experimental values. The analytical expression in Equation 1 can therefore be reliably employed to predict the acceleration response of the marine fender specimens. Figures 5, 6, and 7 also show that the peak accelerations are generally greater for the solid specimens than the hollow ones. This observation is further examined in the next two sections.

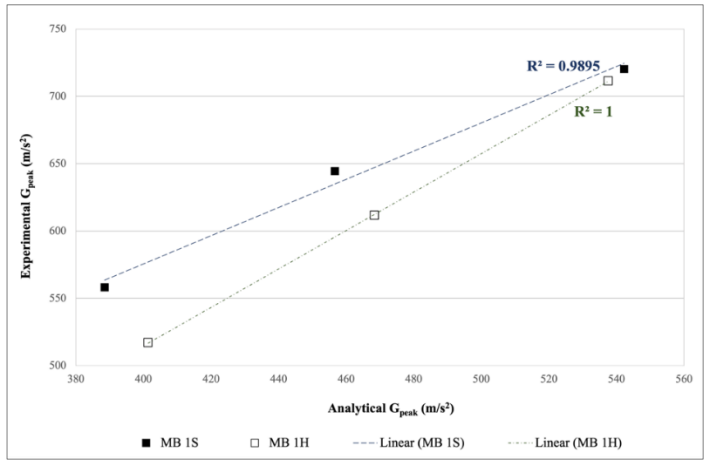

Figure 6: Experimental and analytical shock acceleration responses of specimen MB-1 (t = 10 mm)

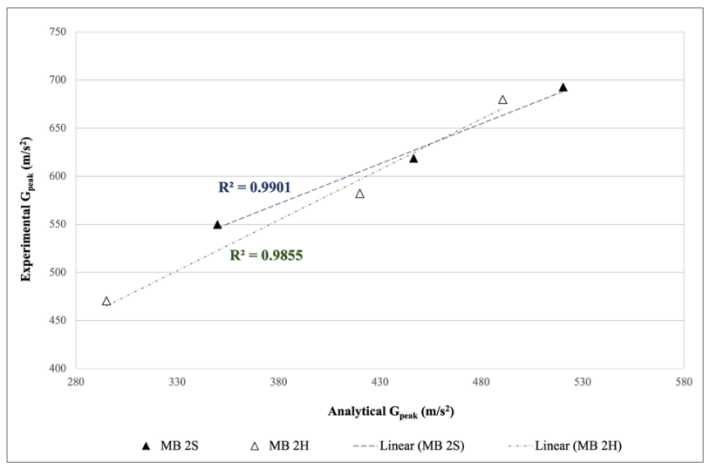

Figure 7: Experimental and analytical shock acceleration responses of specimen MB-2 (t = 20 mm)

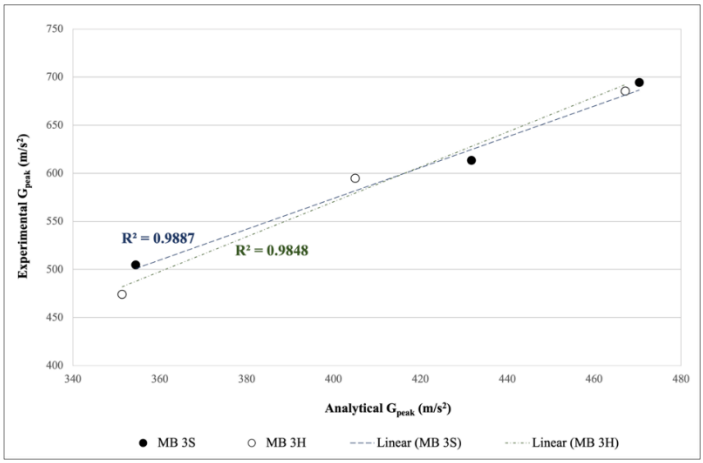

Figure 8: Experimental and analytical shock acceleration responses of specimen MB-3 (t = 30 mm)

Effect of specimen thickness on shock response

The experimentally measured shock responses of the specimens are analyzed based on the effect of their thickness on the resulting peak accelerations. Figures 9, 10, and 11 show the G_{peakEx} values for increasing specimen thicknesses at constant input accelerations of 50G, 60G, and 70G, respectively. It is observed that the G_{peakEx} values decreased for thicker specimens. Since the density and lateral dimensions of all specimens are comparable, thicknesses therefore correspond linearly to specimen masses. This illustrates the effect of increased thickness in lowering the peak acceleration experienced by the specimen. Besides, the pulse durations, dt, are shorter for thicker specimens and at higher input accelerations. Hence the influence of thickness (i.e., mass) on dt and G_{peakEx}, which in turn affects the ensuing impact force and energy absorption capacity of the specimens. These aspects will be discussed in the next two sections.

The effect of reduced mass of the hollow-sectioned specimens of similar thickness on is G_{peakEx} also evident in Figures 9, 10, and 11. G_{peakEx} of the hollow specimens are on average 5% lower than that of the solid specimens for a given thickness and at a given input acceleration. The tubular hollow section thus affected the deformation and energy-absorbing mechanism of the MB specimens. Similar findings for polymeric material systems were reported in [21] and [24]. The effects of the profile and size of through holes on the shock characteristics of MB specimens will be treated in a separate study.

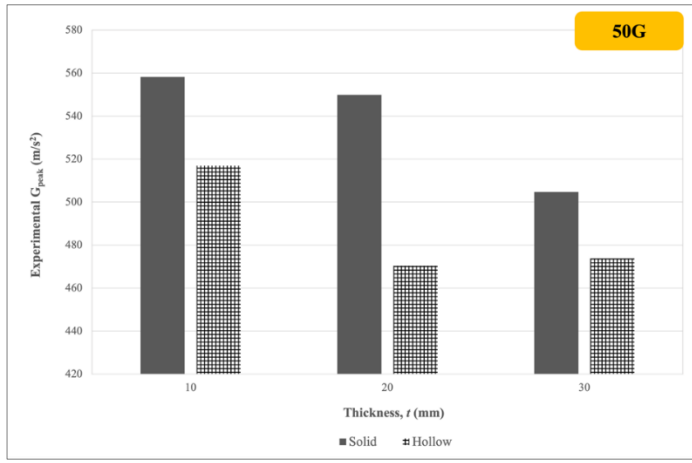

Figure 9: Experimental shock acceleration responses as a function of specimen thickness at 50G input

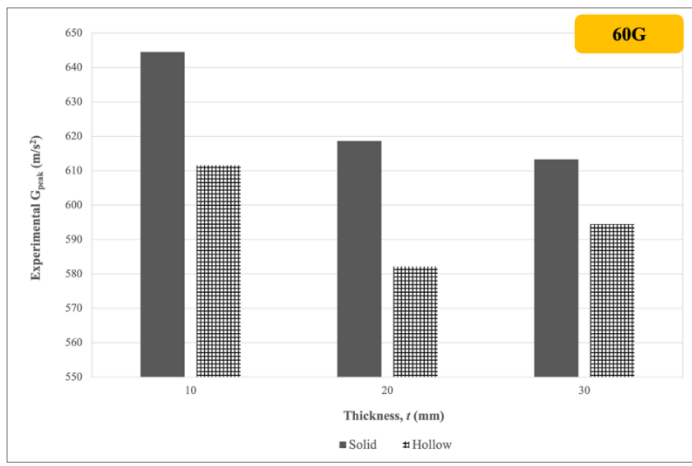

Figure 10: Experimental shock acceleration responses as a function of specimen thickness at 60G input

Effect of velocity change and pulse duration on impact force

Figures 12, 13, and 14 show the analytically determined impact forces at 50G, 60G, and 70G for specimens MB-1, MB-2, and MB-3, in order. The impact forces are calculated using Equation 2 and the experimentally measured velocity change, *dv*, and pulse duration, *dt*. Impact force here is defined as the

force that delivers the shock in a relatively short period of time (i.e., *dt*) when the specimen and the programmer get in contact (see Figure 1b).

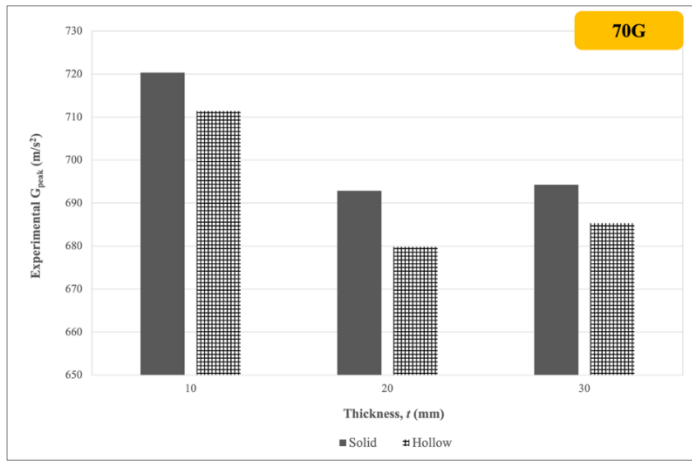

Figure 11: Experimental shock acceleration responses as a function of specimen thickness at 70G input

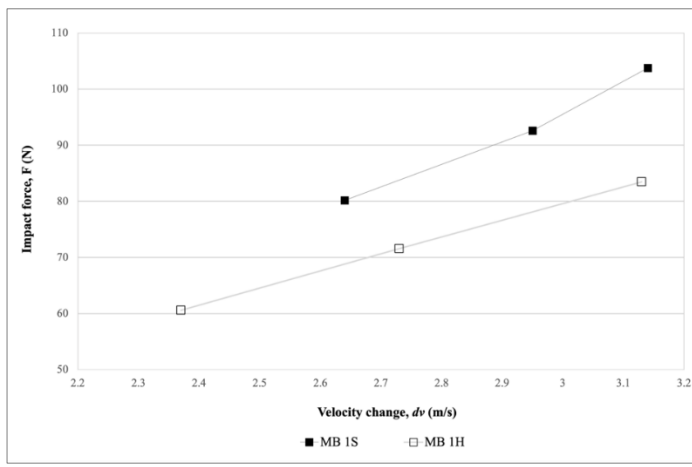

Figure 12: Impact force of specimen MB-1 (t = 10 mm) at 50G, 60G, and 70G

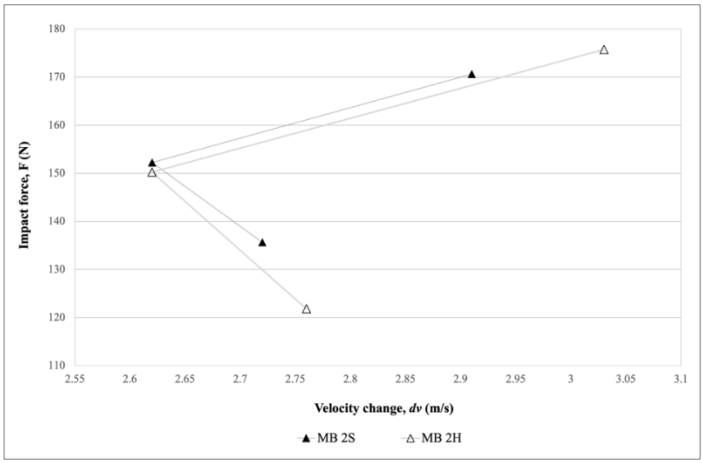

Figure 13: Impact force of specimen MB-2 (t = 20 mm) at 50G, 60G, and 70G

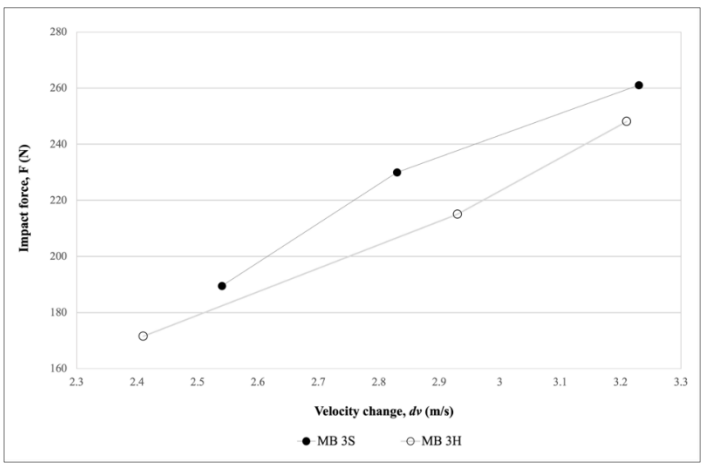

Figure 14: Impact force of specimen MB-3 (t = 30 mm) at 50G, 60G, and 70G

Specimens MB-1 and MB-3 exhibit a linear relationship between dv and the resulting impact force as per Equation 2. However, specimen MB-2, which has a non-uniform mass distribution (see section "Specimen Preparation"), showed a greater inverse dependency on *dt* than its linear relationship with *dv*. In general, impact forces are higher for the solid specimens compared to the hollow specimens. Solid specimens resisted greater

impact forces compared to the hollow specimens as thickness increases from MB-1 to MB-3, which indicates the overriding influence of mass on impact force.

Specific energy absorption

The energy absorbed per unit mass, i.e. specific energy absorption (*SEA*), of the specimens, is determined using Equation 3 and listed in Table 4. The *SEA* of specimens MB-1H and MB-3H are smaller than their solid counterparts by, in order, 11% and 1% on average. Specimen MB-2H, however, has a 6% greater *SEA* than MB-2S. This finding is consistent with that made in section "Effect of specimen thickness on shock response" on the effect of increasing thickness (and thereby, mass) on G_{peak} of MB-2.

Table 4: Specific energy absorption of the marine bumper specimens

Input	Specific energy absorption (J/kg)					
G	MB1-S	MB1-H	MB2-S	MB2-H	MB3-S	MB3-H
50	0.218	0.175	0.231	0.237	0.202	0.181
60	0.273	0.233	0.215	0.215	0.251	0.268
70	0.307	0.305	0.265	0.287	0.325	0.321

The shorter pulse durations for thicker specimens and at higher input accelerations, i.e. greater G_{peakEx} (see section "Experimental and analytical shock acceleration responses"), have an intricate consequence on their *SEA*. Clearly, from Equation 3, larger G_{peakEx} and shorter *dt* will have a leveling net effect on *SEA*. The specimens however registered an average reduction of 30.3% in dt (see Table 2) and a 36.2% increment in median G_{peakEx} (see Figure 5) when the input acceleration is increased from 50G to 70G. This substantiates the higher *SEA* of the specimens at larger input accelerations as can be seen in Table 4. The solid specimens absorbed up to 12% more energy per unit mass than their hollow counterparts. Comparable observations are made in [25]-[27] for a variety of material systems.

Conclusion

The crashworthiness characteristics of an industrial marine fender block are experimentally studied. The as-is test specimen is modified by introducing tubular through-holes to simulate the effects of high acceleration shock experienced by the fender in the real world. Test specimens of 10 mm, 20 mm, and 30 mm thicknesses are subjected to half-sine shock waves for a pulse duration between 5 and 8 ms at desired input accelerations of 50G, 60G, and 70G. Input parameters including drop height and pulse duration (*dt*) that would provide the desired accelerations are identified and validated by correlating the

measured peak acceleration (G_{peakEx}) levels to the theoretically estimated peak acceleration (G_{peakAn}) values. The coefficients of correlation, which lie between 0.9848 and 1, indicate that the analytically determined shock accelerations agree well with that of the experimental values. The combined effects of reduced mass and geometrical change on the G_{peakEx} of the hollow specimens are measured. The specific energy absorption and impact force values of the specimens are then analytically determined. It is found that the through-holes specimens have lower G_{peak} levels, resist smaller impact forces, and absorb up to 12% lesser energy per unit mass than their solid counterparts. This preliminary study also indicates that the impact force of the 20-mm specimen with a non-uniform mass distribution has a greater inverse dependency on dt than its linear relationship with velocity change, dv. Further study will be conducted to investigate the effects of pre-straining and mass distribution on G_{peak}.

Contributions of Authors

The authors confirm the equal contribution in each part of this work. All authors reviewed and approved the final version of this work. David worked on the experimental and data analysis parts alongside with Adelin. Vipin contributed equally on the manuscript drafting and copyreading parts.

Funding

This work received no specific research grant from any funding agency.

Conflict of Interests

All authors declare that they have no conflicts of interest with any party.

Acknowledgment

The authors thank the School of Mechanical Engineering, College of Engineering, Universiti Teknologi MARA, Shah Alam, Malaysia and the Department of Mechanical Engineering, St. Thomas College of Engineering and Technology, Kerala, India for the technical and administrative supports. Malaysia Marine and Heavy Engineering Sdn. Bhd. is thanked for the contribution of the as-is industrial marine fender specimen.

References

[1] X. Guo, J. Deng, and Z. Cao, "Study on the propagation characteristics of pressure wave generated by mechanical shock in leaking pipelines," *Process Safety and Environmental Protection*, vol. 164, pp. 706–714, 2022.

[2] A. M. Asyraf and A. Yulfian, "Rectangular honeycomb structure as absorber structure for road crashed barrier application," *AIP Conference Proceedings*, vol. 2643, no. 1, p. 050068, 2023. https://doi.org/10.1063/5.0110748

[3] V. David and M. Azlan, "Moisture Absorption Properties and Shock Cushioning Characteristics of Bio-Based Polyurethane Foam Composites," *Journal of Mechanical Engineering*, vol. SI 5, no. 2, pp. 157-168, 2018.

[4] Z. Zhang, Z. Xu, X. Shao, Y. Li, and B. Li, "Damage boundary of piezoresistive pressure sensor under shock environment," *Acta Astronautica*, vol. 192, pp. 328–340, 2022. https://doi.org/10.1016/j.actaastro.2021.12.040

[5] D. F. Ledezma-Ramírez, P. E. Tapia-González, M. J. Brennan, and P. J. Paupitz Gonçalves, "An experimental investigation into the shock response of a compact wire rope isolator in its axial direction," *Engineering Structures*, vol. 262, p. 114317, 2022. https://doi.org/10.1016/j.engstruct.2022.114317

[6] F. Mannacio, A. Barbato, F. di Marzo, M. Gaiotti, C. M. Rizzo, and M. Venturini, "Shock effects of underwater explosion on naval ship foundations: Validation of numerical models by dedicated tests," *Ocean Engineering*, vol. 253, p. 111290, 2022. https://doi.org/10.1016/j.oceaneng.2022.111290

[7] Q. Yu, H. Zhang, R. Yang, Z. Cai, and K. Liu, "Experimental and numerical study on the effect of electrohydraulic shock wave on concrete fracturing," *Journal of Petroleum Science and Engineering*, vol. 215, p. 110685, 2022. https://doi.org/10.1016/j.petrol.2022.110685

[8] W. Salman et al., "A high-efficiency energy regenerative shock absorber using helical gears for powering low-wattage electrical device of electric vehicles," *Energy*, vol. 159, pp. 361–372, 2018. https://doi.org/10.1016/j.energy.2018.06.152

[9] W. Li et al., "Magnetorheological semi-active shock mitigation control. Part I: Numerical analysis and preliminary tests," *Journal of Intelligent Material Systems and Structures*, vol. 34, no. 16, pp. 1885-1901, 2023. https://doi.org/10.1177/1045389X221151071

[10] I. Muhammad Zahid, I. Asif Israr, and A. Tanveer, "Semi active control of sinusoidal shock waveform on drop test machine (DTM) using non-

linear dynamic model of hybrid wave generator (HWG) consisting of rubber and electromagnet," *Review of Scientific Instruments*, vol. 94, p. 035005, 2023. https://doi.org/10.1063/5.0124138

[11] M. Spielbauer, P. Berg, J. Soellner, J. Peters, F. Schaeufl, C. Rosenmüller, O. Bohlen, and A. Jossen, "Experimental investigation of the failure mechanism of 18650 lithium-ion batteries due to shock and drop," *Journal of Energy Storage*, vol. 43, p. 103213, 2022. https://doi.org/10.1016/j.est.2021.103213

[12] F. Lei, X. Lv, J. Fang, Q. Li, and G. Sun, "Nondeterministic multi-objective and multi-case discrete optimization of functionally-graded front-bumper structures for pedestrian protection," *Thin-Walled Structures*, vol. 167, p. 106921, 2021. https://doi.org/10.1016/j.tws.2020.106921

[13] Z., Jiang, and M., Gu, "Optimization of a fender structure for the crashworthiness design," *Materials & Design*, vol. 31, no. 3, pp. 1085–1095, 2010. https://doi.org/10.1016/j.matdes.2009.09.047

[14] H. Kawakami, "The use of marine fenders as energy absorbing damper units in mooring systems," in Bratteland, E. (eds) Advances in Berthing and Mooring of Ships and Offshore Structures. NATO ASI Series, vol. 146. Springer, Dordrecht, 1988. https://doi.org/10.1007/978-94-009-1407-0_33

[15] J., Tuleja, K., Kędzierska, M., Sowa, and P. Galor, "Evaluation of the possibility of increasing the energy absorption efficiency of fender devices using the example of cylindrical fenders with additional structural elements applied," *Energies*, vol. 16, no. 3, p. 1165, 2023. https://doi.org/10.3390/en16031165

[16] P. H., Mott and C.M., Roland, "Aging of Natural Rubber in Air and Seawater," *Rubber Chemistry and Technology*, vol. 74, no. 1, pp. 79–88, 2001. https://doi.org/10.5254/1.3547641

[17] Guidelines for design and testing of rubber fender systems (June 2019), Coastal Development Institute of Technology, Japan, 2019. https://www.cdit.or.jp/english/tech/FenderDesignTestGuideline.pdf

[18] R., Iversen, A., Roubos, and P., Mirihagalla, "PIANC Working Group 211: Reliability based design of marine fenders – No more abnormal berthing factor," *American Society of Civil Engineers*, vol. 1, pp. 1435 – 443, 2022. https://doi.org/10.1061/9780784484395.044

[19] H. Taghavifar, A. Modarres Motlagh, A. Mardani, A. Hassanpour, A. Haji Hosseinloo, and C. Wei, "The induced shock and impact force as affected by the obstacle geometric factors during tire-obstacle collision dynamics," *Measurement*, vol. 84, pp. 47–55, 2016. https://doi.org/10.1016/j.measurement.2016.02.003

[20] Y. Liu, T. A. Schaedler, and X. Chen, "Dynamic energy absorption characteristics of hollow microlattice structures," *Mechanics of*

Materials, vol. 77, pp. 1–13, 2014. https://doi.org/10.1016/j.mechmat.2014.06.008

[21] M.A. Mahamood, N. Mohamad, A.R. Jeeffeerie, A.H. Mohd Zain, M.I. Shueb, and H.E. Ab Maulod., "Correlation of open cell structure with properties of green rubber foam from epoxidised natural rubber/reclaimed rubber glove," *Journal of Mechanical Engineering*, vol. SI 1, no. 1, pp. 113-122, 2016.

[22] S. G. Gomez, A. Irigoyen, S. Gonzalez, K. Estala-Rodriguez, E. Shafirovich, Md Sahid Hassan, S. Zaman, and Y. Lin., "Fabrication and characterization of hollow polysiloxane microsphere polymer matrix composites with improved energy absorption," *Journal of Composites Science*, vol. 7, no. 3, pp. 1-18, 2023. https://doi.org/10.3390/jcs7030098

[23] Military Specification (MIL)-STD-810G Test Method 516 (Shock Test), Environmental Engineering Considerations and Laboratory Tests, US Department of Defense, 2008.

[24] K. Szklarek, M. Kotełko, and M. Ferdynus, "Crashworthiness performance of thin-walled hollow and foam-filled prismatic frusta – FEM parametric studies – Part 1," *Thin-Walled Structures*, vol. 181, p. 110046, 2022. https://doi.org/10.1016/j.tws.2022.110046

[25] B. Jiang, X. Chen, J. Yu, Y. Zhao, Z. Xie, and H. Tan, "Energy-absorbing properties of thin-walled square tubes filled with hollow spheres," *Thin-Walled Structures*, vol. 180, p. 109765, 2022. https://doi.org/10.1016/j.tws.2022.109765

[26] A. Sadighi, A. Eyvazian, M. Asgari, and A. M. Hamouda, "A novel axially half corrugated thin-walled tube for energy absorption under axial loading," *Thin-Walled Structures*, vol. 145, p. 106418, 2019. https://doi.org/10.1016/j.tws.2019.106418

[27] J. Li, C. Tian, W. Hong, S. Duan, Y. Zhang, W. Wu, G. Hu, R. Xia, "Shock responses of nanoporous gold subjected to dynamic loadings: Energy absorption," *International Journal of Mechanical Sciences*, vol. 192, p. 106191, 2021. https://doi.org/10.1016/j.ijmecsci.2020.106191

APPENDIX A

Derivation of an expression for peak acceleration, G_{peak}, during shock impact.

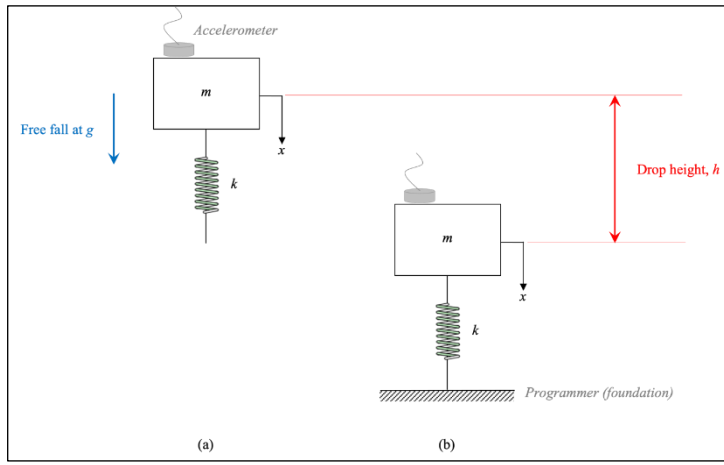

Figure A1: (a) Test specimen during free fall, and (b) test specimen during impact

Free body diagram (at impact)

Note: Static displacement force, $k\Delta$, where Δ is the displacement of the spring from the static equilibrium position (SEP) prior to motion of the system, is balanced by the weight of the mass, mg, i.e $k\Delta = mg$.

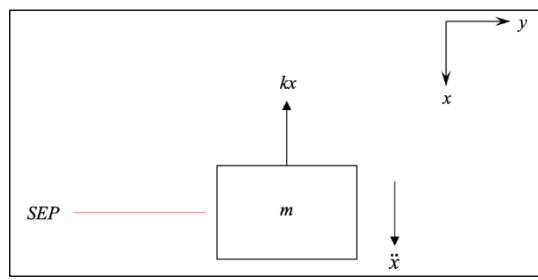

Figure A1: Free body diagram

Equation of motion

Using the Newton's Second Law of Motion:

$$+\downarrow \Sigma F = ma$$

$$\Rightarrow w - k(\Delta + x) = ma \quad : \quad a = \ddot{x}$$

Since $k\Delta = w = mg$,

$$\Rightarrow -kx = m\ddot{x}$$

$$\therefore m\ddot{x} + kx = 0 \tag{1}$$

By applying the definition of natural frequency, $\omega_n = \sqrt{\frac{k}{m}}$ in Equation 1,

$$\therefore \ddot{x} + \omega_n^2 x = 0 \tag{2}$$

Assuming a solution to Equation 2 in the following form:

$$x(t) = A\sin(\omega_n t + \varphi) \tag{3}$$

where A is the amplitude of oscillation and φ is the phase shift between input (impulse force) and output (resulting displacement).

The peak velocity, $\dot{x}_{max}$, and peak acceleration, $\ddot{x}_{max}$, can be obtained from Equation 3 as follows:

$$\dot{x}_{max} = A\omega_n \tag{4}$$

$$\ddot{x}_{max} = A\omega_n^2 \tag{5}$$

Using Equations 4 in 5, the expression of peak acceleration can be rewritten as:

$$\ddot{x}_{max} \equiv G_{peak} = \dot{x}_{max}\omega_n \tag{6}$$

This concludes the basic derivation of an expression for the peak acceleration experienced by the test sample during a shock testing in terms of its peak velocity. The principle of conservation of energy will be invoked next to relate this expression to the test parameters including drop height, h, and pulse duration, dt.

The potential energy, U, of the mass at a height h from where the weight is dropped is assumed to be fully transformed to kinetic energy, T, just as it impacts the programmer at its peak velocity, $\dot{x}_{\max} \equiv v$. In this case,

$$\Rightarrow U = T$$
$$\Rightarrow mgh = \frac{1}{2} mv^2 \tag{7}$$

Rearranging Equation 7 for the peak velocity gives;

$$\therefore v \equiv \dot{x}_{\max} = \sqrt{2gh} \tag{8}$$

Substituting Equation 8 and $\omega_n = \frac{2\pi}{dt}$ where dt is the pulse duration of the impact into Equation 6 yields the final expression of G_{peak} as follows:

$$\therefore G_{\text{peak}} = \frac{\pi\sqrt{gh}}{dt\sqrt{2}} \tag{9}$$

It is to be noted that this expression is subject to the assumption that the system is conservative and there is no rebound of the impactor mass (not the test specimen) during the impact.

Derivation of an expression for specific energy absorption, *SEA*, of the test specimen

Potential energy, U, of the mass at a height h from where the mass is dropped is assumed to be fully transformed to kinetic energy, T, just as it impacts the programmer at its peak velocity (see Figure A1b). Using this assumption, the maximum specific energy absorption of the specimens, SEA, can be determined from the maximum velocity, v_{max}, from Equations 8 and 9 as follows:

$$\Rightarrow T_{max} = \frac{1}{2} m v_{max}^2 \tag{10}$$

$$\Rightarrow SEA = \frac{T_{max}}{m} \tag{11}$$

Substituting v_{max} from Equation 8 into Equation 10 gives:

$$\Rightarrow SEA = \frac{1}{2}(2gh) \tag{12}$$

Substituting gh from Equation 9 into Equation 12 yields:

$$\therefore SEA = \frac{1}{2}\left(\frac{G_{peak} \times dt}{2\pi}\right)^2$$